SLAC-PUB-12291

The LSST camera overview

Kirk Gilmore[1], Steven Kahn[1], Martin Nordby[1], David Burke[1], Paul O'Connor[2], John Oliver[3], Veljko Radeka[2], Terry Schalk[4], Rafe Schindler[1], and the LSST Camera Team

1. Stanford Linear Accelerator Center, P.O. Box 20450, Stanford, CA 94309;
2. Brookhaven National Laboratory, Instrumentation Division, PO Box 5000, Upton, NY 11973.
3. Harvard University, 18 Hammond St., Cambridge, MA 02138.
4. University of California at Santa Cruz, 1156 High St. ,Santa Cruz, CA 95064

ABSTRACT

The LSST camera is a wide-field optical (0.35-1um) imager designed to provide a 3.5 degree FOV with better than 0.2 arcsecond sampling. The detector format will be a circular mosaic providing approximately 3.2 Gigapixels per image. The camera includes a filter mechanism and, shuttering capability. It is positioned in the middle of the telescope where cross-sectional area is constrained by optical vignetting and heat dissipation must be controlled to limit thermal gradients in the optical beam. The fast, f/1.2 beam will require tight tolerances on the focal plane mechanical assembly.

The focal plane array operates at a temperature of approximately -100°C to achieve desired detector performance. The focal plane array is contained within an evacuated cryostat, which incorporates detector front-end electronics and thermal control. The cryostat lens serves as an entrance window and vacuum seal for the cryostat. Similarly, the camera body lens serves as an entrance window and gas seal for the camera housing, which is filled with a suitable gas to provide the operating environment for the shutter and filter change mechanisms. The filter carousel can accommodate 5 filters, each 75 cm in diameter, for rapid exchange without external intervention.

Keywords: Survey, Wide-field, LSST, gigapixel, mosaic

1. INTRODUCTION

The Large Synoptic Survey Telescope (LSST) is a large-aperture, wide-field ground-based telescope designed to obtain sequential images covering the entire visible sky every few nights. The range of scientific investigations which will be enabled by such a survey capability is extremely broad, however in order to optimize the design of the system, we have focused on four main themes: Constraining Dark Energy and Dark Matter, Taking an Inventory of the Solar System, Exploring the Transient Optical Sky, and Mapping the Milky Way. The science requirements imposed by these four themes have significant implications for the technical constraints on the LSST camera, as detailed in this paper:

Constraining Dark Energy and Dark Matter

The primary science drivers for exploring dark energy and dark matter will involve a suite of shear-shear correlation analyses, studies of the shear peak distribution associated with clusters of galaxies, measurements of the galaxy power spectrum and baryon acoustic oscillations, and the use of supernovae as standard candles. The requirements include:

- Coverage of a very large solid angle of sky to faint magnitudes => High system etendue.
- Careful control of PSF shape systematics => Many exposures per field (to reduce atmospheric contributions), active control of optics and the metrology of the focal plane.
- Photometric redshifts out to z ~ 3 => Six-color photometry (ugrizY) with an accuracy better than 1%.
- Well-sampled light curves for detected supernovae => Repeat exposures of each field in multiple colors every few days.

Contributed to SPIE Conference on Ground-Based and Airborne Instrumentation, 5/24/2006-5/31/2006, Orland, FL, USA

Work supported in part by the US Department of Energy contract DE-AC02-76SF00515

Taking an Inventory of the Solar System

The primary science drivers involve the detection of potentially hazardous near-Earth asteroids with diameters > 250 m, and a study of Kuiper Belt Objects down to 26 r mag. The requirements for these investigations include:

- Coverage of most of the sky within +/- 15 degrees of the ecliptic => High system etendue.
- Proper cadence to enable identification of moving objects => Closely spaced pairs of observations 2 or 3 times per lunation.
- Precision determination of orbits => Astrometric accuracy better than 0.1 arcsec.
- Minimization of image trailing => Short exposures, < 15 seconds.

Exploring the Transient Optical Sky

The primary science driver involves the provision of a very large database for studies of multi-color variability of stars, active galactic nuclei, gamma-ray bursts, supernovae, and potentially new transient phenomena on timescales ranging from seconds to years. Requirements include:

- Enhanced probability for the detection of rare events => High system etendue.
- Synoptic time coverage on many different time scales => Short exposures, multiple visits at a variety of cadences.
- Accurate color information for object classification => Six-color photometry with high photometric accuracy.
- Detection of faint variables via image differencing => Control of image systematics, many exposures per field.
- Prompt alerts for follow-up with other facilities => Rapid data processing and object classification.

Mapping the Milky Way

The primary science drivers involves mapping the 3-D shape and extent of our galaxy through photometry, proper motion, and parallax measurements on a variety of distance scales, and the identification and classification of stellar populations on the basis of color and kinematic properties. Requirements include:

- Large area coverage => High system etendue.
- Excellent image quality => Control of systematics, many exposures per field.
- High quality photometry and astrometry => Well-understood system calibration.

These requirements have resulted in the conceptual design of the LSST camera shown in Figure 1.1. It provides a first cut at allocating and sharing space among the components and subsystems. Detailed descriptions follow beginning with the inner cryostat housing, and working outward towards the camera housing.

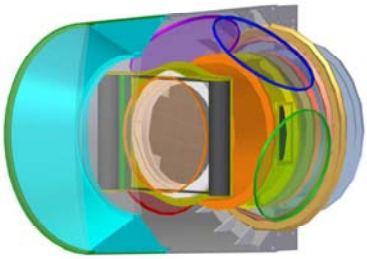

Figure 1.1 Concept-level design of the LSST camera.

2. SENSOR DESIGN

The LSST science goals discussed above lead to a set of challenging performance requirements for the focal plane sensors, listed in Table 2.1:

Table 2.1 Science requirements driving sensor design

Science Requirement	Design Implications
High QE out to 1000nm	thick silicon (> 75 μm)
PSF << 0.7"	high internal field in the sensor high resistivity substrate (> 5 kΩ·cm) high applied voltages (> 50 V) small pixel size (0.2″ = 10 μm)
Fast f/1.2 focal ratio	sensor flatness < 5μm peak-to-valley focal plane package flatness < 10 μm p-to-v package with piston, tip, tilt adjustable to ~1 μm
Wide FOV	3200 cm^2 focal plane > 200-CCD mosaic (~16 cm^2 each) industrialized production process required
High throughput	> 90% fill factor 4-side buttable package, sub-mm gaps
Fast readout	highly-segmented sensors (~6400 output ports) > 150 I/O connections per package

Of central importance are high quantum efficiency (QE) extending into the near infrared and small contribution to the instrument point spread function (PSF) budget. The requirement for high etendue leads to a large focal plane area, which can be economically realized only by using silicon as the sensor material. To achieve high QE in the near-IR, the sensor must be thick because the absorption depth of silicon increases rapidly in this wavelength range. However, increasing detector thickness degrades the spatial resolution of the sensor due to two effects. Diffusion of the photogenerated charge increases because of the longer transit time to the collecting electrode. Thick sensors also require sufficient substrate bias to fully deplete the device; otherwise, lateral diffusion in the undepleted field-free region severely degrades the PSF. A second cause of PSF broadening results from the fast focal ratio of the LSST optics (f/1.2). For red wavelengths where the absorption length is long, the light becomes defocused before it is fully absorbed, further broadening the PSF. Other less pronounced drawbacks of thick sensors include higher dark current and increased contamination from cosmic rays.

Table 2.2 Requirements table (from "The large synoptic survey telescope design and development proposal" submitted to the National Science Foundation by the LSST Corporation, December, 2003)

	Allowable range	Target	Units
Pixel size	8 – 12	10	*m*m
Flatness deviation	10	5	*m*m
Aggregate fill factor (entire array)	90	95	%

Frame read time	3	2	s
Read noise	10	6	e^-
Full well	70000	90000	e^-
Output-output crosstalk	.05	.01	%
Nonlinearity	7	5	%
Dark signal (95^{th} percentile)	4	2	$e^- s^{-1}$
Charge memory (residual image after one readout)	.05	.02	%
QE at 400nm	55	60	%
QE at 600 nm	80	85	%
QE at 800 nm	80	85	%
QE at 900 nm	60	85	%
QE at 1000 nm	25	45	%

3. QUANTUM EFFICIENCY (QE) AND SENSOR THICKNESS

Sensor quantum inefficiencies arise from: *a*) reflection loss, *b*) incomplete charge collection, and *c*) incomplete light absorption. The reflectivity properties of the final LSST sensors will depend on the antireflection coating used on the illuminated surface and on the interface properties of the opposite (charge-collecting) side. Charge collection is expected to be near unity over most of the wavelength range, but surface defects will cause a falloff toward the blue end where absorption takes place very near the surface [1]. For the red and near-IR region, reflection losses will reduce the QE and multiple internal reflections will cause interference fringes in the optical response, Groom *et al*. [2] (although for thick sensors and low f-number the fringing is reduced). The first two causes of QE inefficiency (*a* and *b*) can be reduced by sensor design and processing. The upper limit of QE is determined by *c*) incomplete light absorption, which determines *internal quantum efficiency.*

4. SENSOR FORMAT, READOUT SPEED, READOUT SEGMENTATION AND FABRICATION CONSIDERATIONS

The LSST requirements preclude the use of any existing sensor design. In addition to the need for extended red response and small point spread function (discussed in the previous sections), the fill factor, full well capacity, and readout speed and noise of the sensor have the most impact on LSST science performance. Due to the large (~3200 cm2) imaging area of the focal plane, a large number of individual sensor units will need to be produced, so reliability, reproducibility, and compatibility with industrial fabrication methods are of paramount importance as well [3].

A large format CCD with highly segmented readout is the proposed approach to address these issues. Large format will minimize the number of gaps between sensors in the assembled mosaic. To provide for a 2 second readout of the entire focal plane, it will be necessary to have multiple outputs per CCD operating in parallel. As the number of outputs per CCD is increased, the readout speed per output can be reduced, thus minimizing the noise bandwidth. However, a correspondingly higher number of electronic signal processing channels will be required. Output-to-output crosstalk must be minimized, and reaching the required level is expected to be a challenge for the electronics development.

A further advantage of segmentation is that it can be used to reduce the impact of bloomed charge from bright stars. In a 15-s LSST exposure the charge from 16^{th} magnitude and brighter stars will exceed the pixel full well capacity, resulting in blooming up and down the column. By choosing an appropriate segmentation the length of the affected columns can be kept small, so that blooming from a saturated star is contained to within no more than .005% of the imaging area. Segmentation also substantially reduces the power dissipation of the clock drivers.

It is assumed that the LSST sensors will be developed and produced by a commercial vendor or vendors. However, using expertise that exists within the collaboration a "strawman" design of a large format, highly segmented CCD design has been produced, which is discussed in detail in the next section. The geometries of the frontside electrodes have been chosen to be consistent with today's production CCD technology. It is anticipated that this strawman design can be used as a starting point for negotiations with potential CCD vendors leading to a contract for the production of the first prototypes.

4.1 CCD Strawman design outline

The overall features of the strawman sensor design are listed in Table 4.1:

Table 4.1 Sensor features

Parameter	***Value***
Pixel size	*10 mm*
Format	*4000 × 4000 pixels*
Segmentation	*Eight 4000 × 500 pixel sub-arrays, 4 outputs each*
Total no. of output amplifiers	*32*
Anticipated gain	*3 – 5 mV/e^-*
Parallel clocking	*4-phase (4 poly layers)*
Serial clocking	*3-phase*
Contiguous column length:	*500 pixels (100 arcsec)*
Guard ring	*100 mm*
Pin count	*208*
Fill factor	*96.5%*

We chose the 4k x 4k format to be the largest footprint consistent with good yield. Each amplifier will read out 500,000 pixels (one-quarter of a 4000 × 500 sub-array), allowing a pixel readout rate of 250 kHz per amplifier. The gaps between sub-arrays are approximately 100 mm. In image space, therefore, the sub-arrays are 13.3 arcmin long by 1.67 arcmin wide, with gaps of 2 arcsec separating them in the long dimension.

The strawman CCD architecture is illustrated in Figure 4.1 All pins are located along the two side edges. Shared serial and parallel metal busses connect the respective clock phase lines together.

The design was accomplished using a single metal layer, in order to demonstrate compatibility with as broad a range of fabrication facilities as possible. There are a few benefits to be had in reduced pinout and reduced drive impedance by going to a 2-metal process. Also, there are minor improvements in pinout and fill factor by changing to a 2-phase serial structure if this can be accomplished without greatly increased risk of incomplete charge transfer.

5. HYBRID SILICON PIN-CMOS

The other candidate sensor type is a hybrid device consisting of a thick, high resistivity silicon photodiode array bump-bonded to a CMOS readout ASIC, referred to as a "Si PIN-CMOS sensor"[3]. A hybrid PIN-CMOS sensor has a sandwich construction consisting of a pixilated photodetector layer bump-bonded to a CMOS multiplexer integrated circuit, as illustrated in Figure 5.1. In this sense it is similar to hybrid near-IR array sensors that have gained wide acceptance in the IR astronomical community. Separation of photon detection from readout facilitates independent optimization of the Si PIN detector array and of the CMOS readout electronics. Bump bonding between the two planes of contacts with a pixel size as required for LSST (~10 μm) presents a technological challenge (18 μm pitch has been achieved). The bias on the PIN array is in the 30–50 V range depending on the thickness (the considerations on the thickness, depletion and diffusion apply equally as for CCDs). Virtually all the charge resulting from photon conversion is collected on pixel electrodes (implants), and thus this sensor approaches 100% fill factor over the sensitive area. An area has to be provided at the edges of the sensor for the guard rings required to sustain the bias.

The CMOS readout contains a sense amplifier and a reset transistor in each pixel. The readout ("multiplexer") is arranged in a matrix of (row) select lines and (column) sense lines. In a normal readout mode pixels are addressed row by row. The columns provide information in parallel for a row of pixels, and this information is multiplexed to a number of outputs determined from the readout speed requirements. A variety of windowed readout modes may be obtained by utilizing flexible addressing controls in the multiplexer.

The reset transistors at each pixel (normally driven row by row), can also perform the function of an electronic shutter, eliminating the mechanical shutter needed for a CCD array. The resulting improved system reliability is a significant advantage of this type of sensor.

Evaluation of Si PIN-CMOS devices for scientific applications such as LSST is still at an early stage. Devices with 18 μm pixels, and with a smaller overall format, have been undergoing tests. Quantum efficiency was found to be as expected for the PIN layer thickness used, and the dark current was lower than required. The read noise for single CDS samples exceeds LSST requirements at present, and will be further studied. Devices with large formats and small (10 μm) pixel size are in active development by at least one manufacturer. Monolithic CMOS imagers, another CMOS-based technology, have not as yet achieved low-light performance suitable for astronomy. They have a very thin active region (a few μm), and a fill factor «100%.

.

6. FOCAL PLANE ELECTRONICS

6.1 General Discussion

The LSST Focal Plane represents a quantum leap in size and scope over those in use in telescopes today. While both CMOS/PIN diode image sensors and CCDs remain under consideration, we restrict our attention here to the CCD option, the readout electronics support 4K X 4K CCD sensors with 32 output ports per device. With the exception of the Front End Module, comprising the front end signal processing electronics, the remaining downstream electronics could accommodate a CMOS image sensor array as well.

The combined requirements of large size, high dynamic range, low noise, and rapid readout time, dictates a highly segmented focal plane with about 6,400 readout ports. This, in turn, dictates a high degree of integration for both the "front end" electronics, those which process the CCD output signals and provide clocks, as well as the "back end" which digitizes the data, buffers it, and sends it off-camera via optical fiber.

The entire LSST focal plane is synchronous in operation, which means that clocking for all sensors in the array is synchronous to the level of some tens of nanoseconds. This assures repeatability and robustness against feedthrough and pickup. Timing generation takes place within the Timing/Control crate under command from the off-camera control system.

The structure of both front end and back end electronics follows the "raft based" distribution of image sensors. A raft refers to a 3x3 array of sensors constrained to a common mechanical structure. The raft structure consists of 9 imagers each which has 32 segments for a total of 288 CCD output ports (source followers).

Specifications for the LSST Focal Plane and Readout are shown below in Table 6.1.

Table 6.1 Focal plane array and readout specifications

Parameter	Value
FPA size	~3.5 gigapixels
Number of CCD sensors	~200
Pixel size	10 μm × 10 μm
CCD size	4k × 4k
CCD output ports	32 ports, 500,000 pixels each
Total no. output ports	~6,400
Full well capacity	100,000 e^-
Read noise	6 e^- rms
Dynamic range	16 bits
Readout time	2 s
Nominal exposure time	15 s

7. FOCAL PLANE COMPONENTS AND LAYOUT

7.1 CCD Packages

Each sensor chip is attached to a support structure consisting of materials with very low and matched temperature expansion coefficients, such as aluminum nitride and invar. Such a package is shown schematically in Figure 7.1.1 and Figure 7.1.2. It consists of a 4-side buttable silicon detector glued to an aluminum nitride substrate. Bond wires then make the electrical connection between the photon-sensitive silicon and metal pads on the aluminum nitride. The metal lines route electrical connections to two connectors.

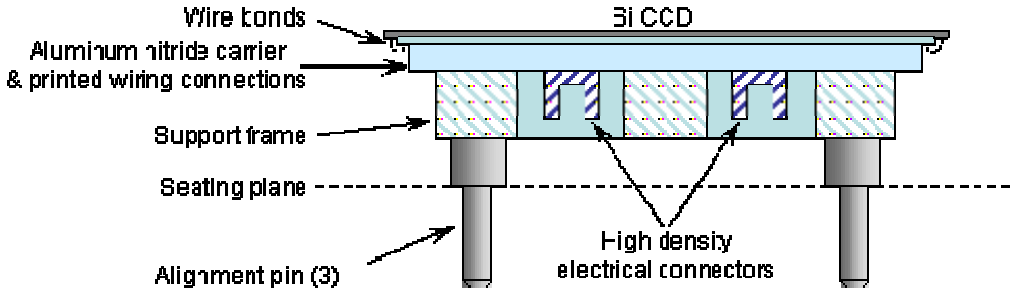

Figure 7.1.1 Proposed sensor package showing a CCD on aluminum nitride carrier with electrical and mechanical interfaces.

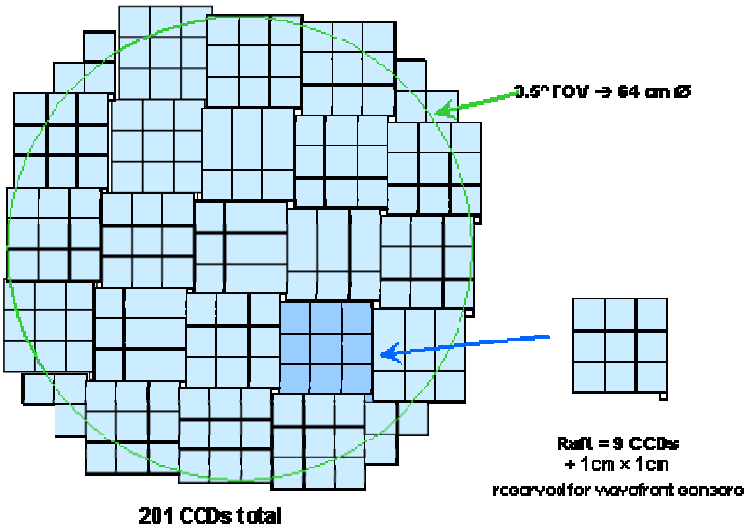

Figure 7.2 An example of a 3x3 sensor sensor rafts in the focal plane with areas provided for wavefront sensors by raft offset.

7.2 Integrating structure

The rafts are assembled and tested with front-end electronics, as illustrated in Figure 7.3.1. These raft assemblies are then installed in an integrating structure. The physical space between sensors is minimized to maximize sensitive area ("fill factor"), yet contact must be avoided to avoid permanent damage. If the guide pin technique used to assemble individual sensor packages into rafts is inadequate for installing rafts into the integrating structure, an assembly fixture will be designed and built and a procedure developed to facilitate routine insertion. This fixture would be moved to the telescope site so any faulty sensors could be replaced with spares.

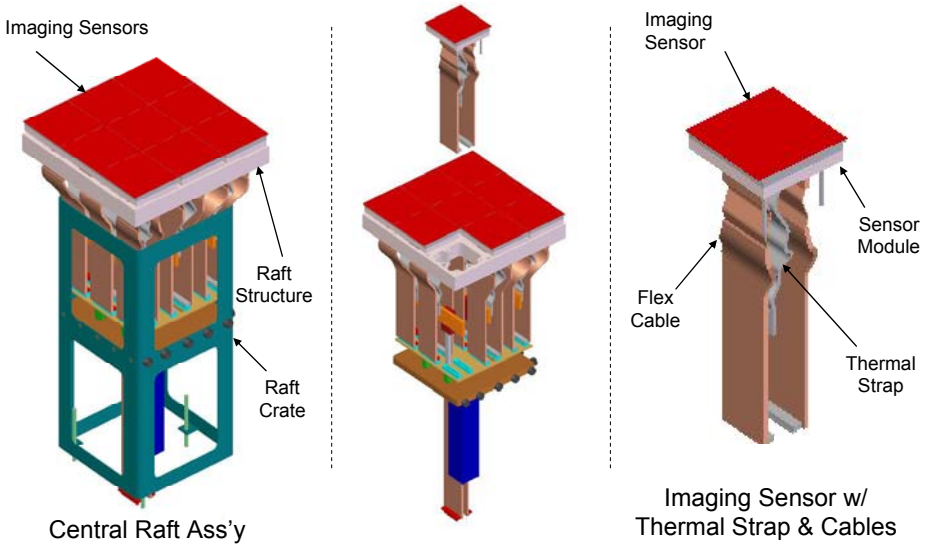

Figure 7.2.1 Raft module with integrated front-end electronics and thermal connections.

7.3 Focal Plane Flatness

Achieving 10 μm peak-to-valley flatness over the whole focal plane array is challenging because there are several error contributors needing to be of order 1 μm or less. The error budget, which apportions flatness and size tolerances among components (e.g., individual sensors, rafts and integrating structure) and changes that occur in interfaces and components with time, temperature and orientation, is coupled with the approach for building the array. For example, all components can be manufactured with sufficient precision to assemble in snap-together fashion without needing adjustments, but this may be more expensive than providing relatively few simple adjustments to relax difficult tolerances. The final choice will depend on analysis and testing results and on interactions with sensor vendors,

There are 201 sensors in the focal plane array, each with three mounting pads. This is a sufficient number to favor developing an industrial process with sufficient precision to avoid custom manufacture or adjustments. This preference is reflected in the error budget, which allocates 5 μm peak-to-valley height tolerance to the sensing surface with the sensor mounted to a perfect plane. Therefore, individual sensors must be sufficiently flat, parallel and at the same height after mounting to achieve 5 μm peak-to-valley

Arrays of 3 X 3 sensors are mounted to raft structures that in turn mount to the integrating structure. Raft structure plates can be double-side lapped all at once to be flat, parallel and the same size to less than 1 μm. Thus, rafts assembled with sensors should be flat, parallel and the same height to 6.5 μm peak-to-valley.

A 5 X 5 array of rafts mount to the integrating structure in a similar manner as the sensors with three coplanar pads, giving 75 pads total. These mounting pads incorporate flexural freedom to avoid over-constraint of thermal expansion, which could alter the flatness of rafts and the integrating structure and be potentially damaging. The integrating structure can be manufactured flat to 1 μm at room temperature and it can be made stiff enough to deflect less than 1 μm due to the changing orientation of the telescope.

8. THERMAL CONTROL SYSTEM

The Camera Thermal System (CTS) is shown schematically in Figure 8.1. It is primarily integrated within the LSST camera body but transfer lines for the connections to refrigeration and vacuum system components are expected to penetrate the camera body and be extended through the telescope structure to the observatory hall. Control lines also follow a similar path.

The cryostat contains a complex package of components and subassemblies shown. The primary heat sources that must be addressed are the on-chip sensor readout electronics, radiation through L3 onto the FPA, the front end and back end electronics and the warm inner surfaces of the cryostat body. In addition there are a modest number of structural supports, penetrations and feed-thru connections providing conductive paths to the outer camera body and N2 environment.

The back end electronics modules are also located at the back of the cryostat and in the cryostat vacuum. Heat from these back-end electronics is removed by a second circuit of liquid, cooling a second heat-sink plate. The BEE units are connected to the rafts by flexible cables penetrating both cold plates.

To insure that the FPA remains optically clean, the cryostat is divided into three distinct vacuum regions that are quasi-isolated, allowing us to minimize the migration of contaminants by molecular flow onto the cold sensor surface during cool down, warm up and while in operation.

Most of the liquid refrigeration system is located off of the camera assembly, and the telescope to reduce vibration and thermal sources. Some passive vacuum pumping and monitoring capability is likely to be provided within the camera body.

9. CORRECTOR OPTICS AND COLOR FILTERS

9.1 Introduction

The LSST camera optics [4] consist of 3 fused silica lenses with diameters of 1.6 m, 1.1 m and 0.73 m that correct for field aberrations, along with interchangeable filters with diameters of 0.78 m that give spectral coverage from the UV to near IR, in 5 broad bands. The three lenses along with 0.64 m diameter detector array are housed in a canister, ~ 1.6 m in diameter, the size of the largest lens, as shown in Figure 9.1.1.

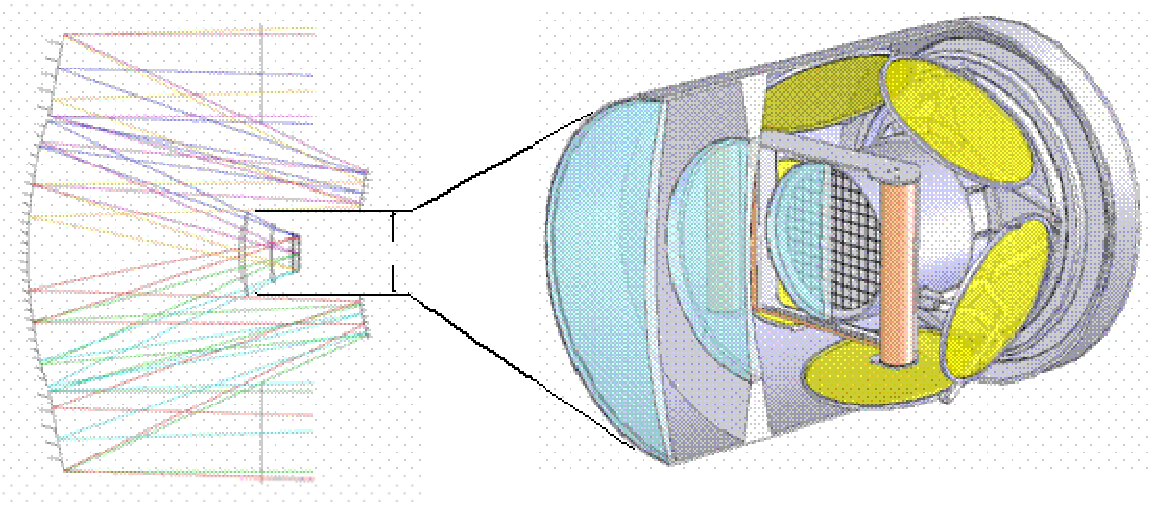

Figure 9.1.1 The optical design defines the size and placement of the optical elements and ray bundles define stay-out zones for support hardware. This concept-level design of the LSST camera shows three corrector optics, storage of five color filters, the focal plane array and other camera hardware.

9. FILTER SET

The current LSST baseline design [4] uses a filter set comprised of standard astronomical u, g, r, i, z, and Y bands. The goal of 1% relative photometry in LSST images defines the general feature of the LSST filter set and is detailed below.

The LSST filter set has been based on the SDSS filter set which is known to have the desired characteristics that are required for the LSST filter set.

Approximate FWHM transmission points are shown in Table 9.1.

Table 9.1 Baseline LSST filter band-pass FWHM points.

Filter	λ_1	λ_2
u	330	400
g	402	552
r	552	691
i	691	818
z	818	922
Y	970	1060

LSST Design Parameters:

1. Beam that is incident on the filter has a focal ratio of f/1.25 with a 61.5% obscuration.

2. The filter is concentric about the chief ray so that all portions of the filter see the same angle of incidence range, about 14.2º to 23.6º

The LSST filter set was modeled using the total system throughput including atmospheric extinction, mirror reflectivities, lens transmissivities, and detector quantum efficiency and is shown in Figure 9.1.

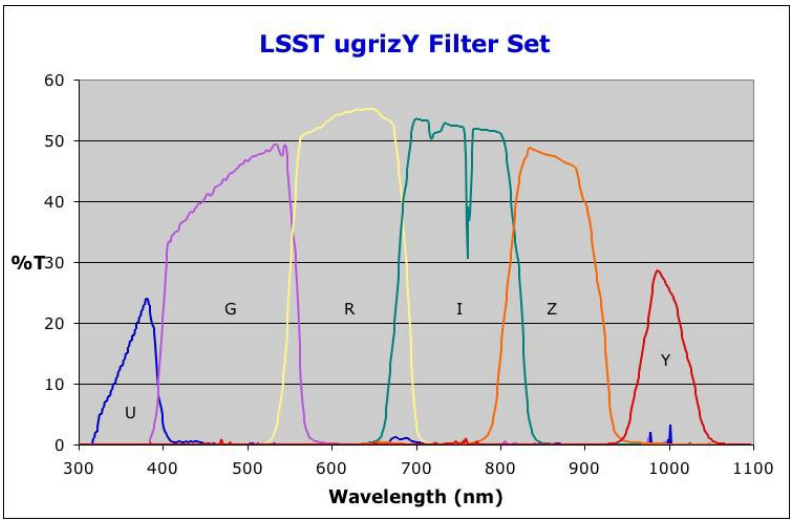

Figure 9.1 LSST Filter Set

10. CONTROLS AND DAQ

10.1 Design Approach and Logical Structure

The camera comprises the last stages of the optical system, the sensors to convert light to digitized images, and the hardware and software to transfer the images into the LSST data management system. The Camera Control System (CCS) manages the activities of the various camera subsystems and coordinate those activities with the Observatory Control System (OCS). The CCS comprises a set of modules (nominally implemented in software) which are typically responsible for managing one camera subsystem. In this section, a logical (or symbolic) view of the CCS is presented followed by discussion of the various camera subsystems and their corresponding control modules. Finally a short discussion of the data acquisition system and the interface to data management is presented.

The approach we are following parallels the current OCS model. We assume that a single control module manages a camera subsystem. Generally, a control module is a long lived "server" process running on an embedded computer in the subsystem. Multiple control modules may run on a single computer or a module may be implemented in "firmware" on a subsystem. In any case, control modules must exchange messages and status data with a central control module (CCM). The main features of this approach are:

1. Control is distributed to the local subsystem level where possible and time critical loops are closed at the local level
2. The systems follow a "Master/Slave" strategy with one CCS module (CCM) acting as the master
3. Coordination will be achieved by the exchange of messages through the interfaces between the CCS and its subsystems.

Acknowledgements

The LSST design and development activity is supported by the National Science Foundation under Scientific Program Order No. 9 (AST-0551161) through Cooperative Agreement AST-0132798. Portions of this work were performed in

part under Department of Energy contracts with the Stanford Linear Accelerator Center under contract DE-AC02-76SF00515, with Brookhaven National Laboratory under contract DE-AC02-98CH10886, and with Lawrence Livermore National Laboratory under contract W-7405-ENG-48
Additional funding comes from private donations, in-kind support at Department of Energy laboratories and other LSSTC Institutional Members."

References

1. P. O'Connor et al., "Study of Silicon Sensor Thickness Optimization for LSST", Proc. SPIE, 6276-75, 2006. In Press
2. D. E. Groom et al., "Quantum efficiency of a back-illuminated CCD imager: An optical approach," Proc. SPIE, vol. 3649, pp. 80–90, 1999
3. J.C. Geary et al., "The LSST Sensor Technologies Studies, Proc. SPIE 6276-01, 2006. In press.
4. S. Olivier et al., "LSST Camera Optics", Proc. SPIE, 6273-33, 2006. In press.
5. S. Marshall, et al., "LSST Camera Control System", Proc. SPIE, 6274-75, 2006. In press.

Members of the LSST Camera Team

Sam	Aronson	BNL	Martin	Perl	SLAC
Steve	Asztalos	LLNL	John	Peterson	SLAC
Kevin	Baker	LLNL	Don	Phillion	LLNL
Gordon	Bowden	SLAC	Veljko	Radeka	BNL
Pat	Burchat	Stanford	Andy	Rasmussen	SLAC
David	Burke	SLAC	Dave	Rich	SLAC
Chuck	Buttehorn	BNL	Leslie	Rosenberg	Washington
Nathan	Felt	Harvard	Terry	Schalk	UCSC
Don	Figer	STScI	Rafe	Schindler	SLAC
Mike	Foss	SLAC	Lynn	Seppala	LLNL
James	Frank	BNL	Lance	Simms	SLAC
John	Geary	CFA/Harvard	Chris	Stubbs	Harvard
Perry	Gee	UC Davis	Pete	Takacs	BNL
Kirk	Gilmore	SLAC	Jon	Thaler	UCUI
Gary	Guiffre	SLAC	Tony	Tyson	UC Davis
John	Haggerty	BNL	Richard	Van Berg	U. Penn
Layton	Hale	IMS	Brian	Winer	Ohio-State
Klaus	Honscheid	Ohio-State	Wayne	Wistler	LLNL
Mike	Huffer	SLAC	Tom	Weber	SLAC
Richard	Hughes	Ohio-State			
Garrett	Jernigan	UCB/SSL			
Steven	Kahn	SLAC			
Peter	Kim	SLAC			
David	Kirkby	UC Irvine			
Phil	Kuczewski	BNL			
Ted	Lavine	SLAC			
Eric	Lee	SLAC			
Steffen	Luitz	SLAC			
Stuart	Marshall	SLAC			
Morgan	May	BNL			
Mitch	Newcomer	U. of Penn			
Martin	Nordby	SLAC			
Paul	O'Connor	BNL			
John	Oliver	Harvard			
Scot	Olivier	LLNL			

BNL = Brookhaven national Laboratory
LLNL = Lawrence Livermore Natinal Lab
SLAC = Stanford Linear Accelerator Center
UCB = University of California Berkeley
UIUC = University of Illinois Urbana
UCSC = University of California at Santa Cruz